Self-oscillations of domains in doped GaAs-AlAs superlattices

J. Kastrup, R. Klann, H. T. Grahn, and K. Ploog
Paul-Drude-Institut für Festkörperelektronik, Hausvogteiplatz 5-7, D-10117 Berlin, Germany

L. L. Bonilla, J. Galán, M. Kindelan, and M. Moscoso
Escuela Politécnica Superior, Universidad Carlos III de Madrid, Butarque 15, E-28911 Leganés, Spain

R. Merlin
The Harrison M. Randall Laboratory of Physics, The University of Michigan, Ann Arbor, Michigan 48109-1120
(Received 31 May 1995)

Self-sustained oscillations of the current have been observed and simulated in a doped GaAs-AlAs superlattice under voltage control. Depending on the applied bias the detected frequencies vary between 250 kHz at low voltages and 20 MHz at high voltages. Amplitude and frequency decrease with increasing carrier density until, at very high excitation densities, stable electric-field domains are formed. A discrete drift model reproduces the current oscillations and shows that they can be attributed to the spatial oscillation of the boundary between the two domains.

Since the discovery of Bloch oscillations in semiconductor superlattices (SL's) a few years ago, the subject of electric-field domains in SL's has become increasingly important. In order to realize a device based on Bloch oscillations, a certain degree of doping is necessary in such a system. However, doped superlattices exhibit the formation of electric-field domains. These domains appear as a consequence of the strongly enhanced tunneling probability at field strengths, where subbands of adjacent wells are at resonance, in conjunction with a large carrier density.[1–3] The applied electric field breaks up into two distinct field domains with a charged boundary layer. As the applied voltage is increased the domain boundary moves through the SL well by well with each step leading to a sharp discontinuity in the current-voltage (I-V) characteristic. Between the discontinuities the current evolves along stable branches with each branch corresponding to a unique location of the domain boundary. For a given bias value the charge boundary may be centered in different wells of the SL leading to a multistability of the I-V characteristic.[4]

Electric-field domain formation has also been investigated in undoped superlattices introducing electron and hole densities by photoexcitation. Two well-separated photoluminescence (PL) lines have been observed identifying the two field domains by their Stark shift.[5] Recently, time-resolved experiments using a steplike laser excitation revealed damped current oscillations in the MHz range.[6] These oscillations have been attributed to a periodic movement of the domain boundary over several periods.[7] Damped Gunn oscillations induced by intense picosecond light pulses have been observed in strongly coupled undoped SL's.[8]

In this paper we present the observation and simulation of undamped self-oscillations of the current in *doped* GaAs-AlAs superlattices. The frequency of the oscillations can be reduced by further increasing the carrier density through optical excitation. At very large carrier densities the oscillations disappear completely resulting in the well-known series of stable current branches. The calculations reveal that the current oscillations are due to a motion of the domain boundary over several periods.

The investigated SL sample has 40 periods of 9-nm GaAs wells and 4-nm AlAs barriers grown on a [100] n^+-type GaAs substrate. The central 5 nm of each well have been doped with Si donors leading to a two-dimensional electron density of $n_{2D} = 1.5 \times 10^{11}$ cm^{-2}. The SL is sandwiched between two highly Si-doped n^+-type $Al_{0.5}Ga_{0.5}As$ buffer layers forming an n^+-n-n^+ diode. The samples have been processed into mesas of 120-μm diameter. The data have been recorded at 5 K with the sample mounted on the cold finger of a He-flow cryostat. For the I-V measurements we used a Hewlett-Packard (HP) 3245A voltage source and a HP3458A multimeter to record the current. The current oscillations have been detected with a HP54720A digital oscilloscope. The experiments with optical excitation of additional carriers have been performed using an intensity stabilized Ti:sapphire laser.

Current-voltage (I-V) traces without and with illumination are shown in Fig. 1(a). Note that only the voltage sweeps towards higher fields are displayed, in contrast to Ref. 4. The dark current clearly shows two plateaulike regions, which is typical for domain formation. However, the fine structure associated with the period-by-period motion of the domain boundary is missing. The latter is recovered for strong illumination as shown in the upper trace. In the lower plateau the two domain field strengths are related to resonant tunneling between the lowest electronic subbands ($C1C1$) and resonant coupling between the lowest and the second electronic subband ($C1C2$) in adjacent wells. The second plateau begins at a bias voltage at which the whole SL is in $C1C2$ resonance. The high-field domain in the second plateau has not yet been identified.

In order to understand the dark I-V characteristic,

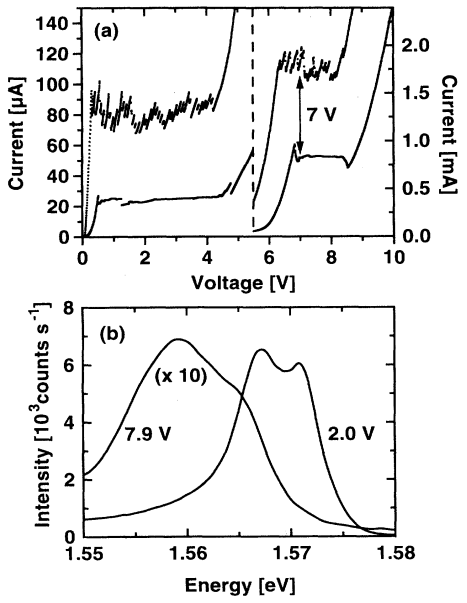

FIG. 1. (a) I-V characteristic of the sample at 5 K. The upper curve has been recorded with a laser power of 500 mW (1.653 eV). The left half of the plot was multiplied by a factor of 16. (b) PL spectra at 5 K from the plateau regions at an excitation power of 10 μW (1.653 eV). The spectrum at 7.9 V has been rescaled by a factor of 10.

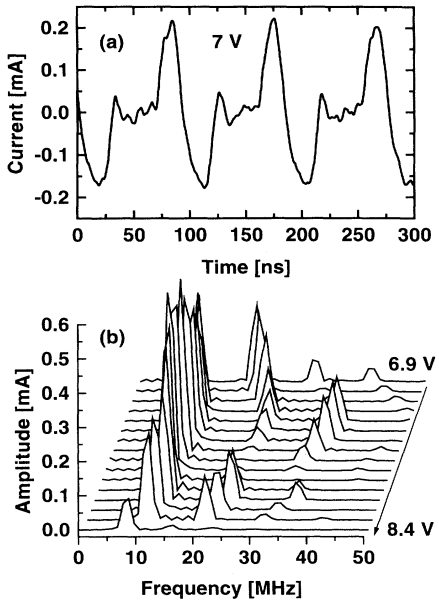

FIG. 2. (a) Typical trace of the time-resolved current at 7 V with a dc average of 0.8 mA at 5 K. (b) Fourier transforms of the dark current oscillations vs frequency for different applied voltages (0.1-V steps) in the upper plateau.

PL experiments have been performed in both plateau regions. The PL spectra have been recorded at very low laser power leaving the I-V characteristic unchanged. Nevertheless, in both plateau regions the PL spectra display two peaks at fixed energetic positions, which change their relative intensity with increasing bias. Examples for two selected voltages are shown in Fig. 1(b). The spectra are typical for electric-field domain formation in SL's, even though the I-V characteristic does not show the expected fine structure. This observation suggests that two field domains are present, but their spatial distribution is not stable. At large laser power [upper curve in Fig. 1(a)] the PL spectra become very broad and the two PL lines cannot be resolved.

In Fig. 2(a) the time-resolved current is shown for an applied voltage in the second plateau region. A periodic oscillation of the current with time in the nanosecond regime is clearly observed. It is apparent from Fig. 2(a) that the oscillation is not purely sinusoidal, but contains higher harmonics. The fundamental frequency of the oscillations is typically 10 MHz in the upper plateau and 0.25 MHz in the lower plateau region. Because the oscillation amplitude is much larger in the upper plateau, we will focus on this region. Since the data points in the I-V characteristic represent an average over many oscillation periods, no structure is present in the plateau regions of Fig. 1(a), although the PL measurements clearly show that two distinct domains are existent. In Fig. 2(b) we plot a series of Fourier transforms of the current oscillations for applied voltages in the upper plateau regime without illumination of the sample. The Fourier transforms disclose that the current oscillations contain a fundamental frequency of 10 MHz and several higher harmonics. While the positions of the peaks do not change much with voltage, the intensity distribution among the peaks changes rather drastically. At 6.9 V the largest frequency peak is at about 20 MHz. With increasing voltage this peak decreases, while the intensity of the 10- and the 30-MHz peaks diminishes until, at about 7.9 V, the trend is reversed.

As shown in Fig. 1(a) the I-V characteristic changes drastically when additional carriers are introduced. The oscillatory behavior as a function of laser power is shown in Fig. 3. The Fourier transforms of the current oscillations are given for laser intensities between 10 and 500 mW at an applied bias of 7 V. This voltage was selected from the first half of the plateau, because the plateau shifts to smaller voltages with increasing laser power [see Fig. 1(a)]. Above 150 mW the fundamental frequency de-

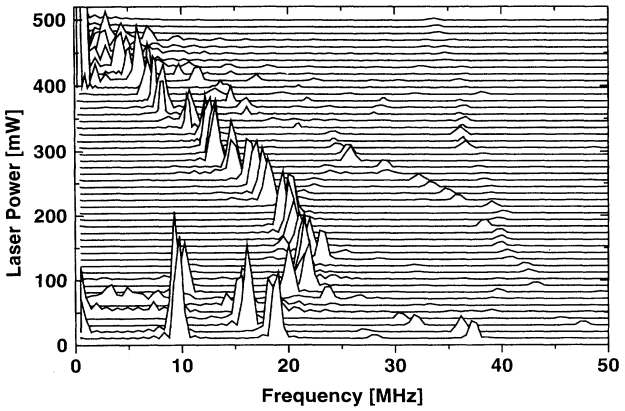

FIG. 3. Fourier transforms of the current oscillations at 7 V as a function of laser power (1.569 eV) at 5 K.

creases linearly with laser power towards lower frequencies until, at about 500 mW, the oscillations disappear. The slope is -7 MHz/100 mW for the fundamental frequency, while the second harmonic has twice the slope.

These results can be understood within a discrete drift model recently introduced by Bonilla *et al.*[7] taking into account the doping of the wells and the n^+-n-n^+ structure of the present sample. We consider a set of weakly interacting quantum wells characterized by average values of the electric field E_j and carrier densities n_j (electrons) as well as p_j (holes) with $j = 1, \ldots, N$ denoting the well index. This mean-field-like approach is justified because the relevant time scale for the oscillations (~ 0.1 μs) is much larger than those for the tunneling process between adjacent wells (~ 0.5 ns) and the relaxation from excited levels to the ground state within each well (~ 0.5 ps). The one-dimensional equations governing the dynamics of the system have been described in Ref. 9, where the doping density N_D has been incorporated into the equations of Ref. 7. The boundary condition $\epsilon(E_1 - E_0)/(el) = n_1 - p_1 - N_D = \delta$ allows for a small negative charge accumulation in the first well, which is taken to be $\delta \sim 10^{-5} \times N_D$. The physical origin of δ is clear: Due to the different electron concentrations at each side of the first barrier, some charge will be transferred from the contact to the first quantum well. This creates a small dipole field, which cancels the electron flow.

The model equations of Ref. 9 have been solved in dimensionless units using the experimental values of Fig. 1 as a reference. We take the average doping density N_D (1.15×10^{17} cm^{-3}) per SL period as the unit of electron and hole density. The applied voltage at the first resonant peak in the current-voltage characteristic, i.e., about 6.8 V, is adopted as the voltage unit. The unit of time (28 ns) is set by normalizing the electron velocity at the first resonant peak (467 cm/s) to 1 in units such that the average permittivity and the SL period are 1. With these values the unit of current is about 1 mA and the unit of frequency is 36 MHz. In Fig. 4 we plot the calculated current versus the applied voltage for a dimensionless doping density of $\nu = 0.1$ for three different laser powers ($\gamma = 0$, 1×10^{-2}, and 4×10^{-2}). These curves were obtained using the drift velocity versus field characteristic shown in the inset of Fig. 4. The calculated current without photoexcitation exhibits oscillations as observed in the experiment. The time-integrated I-V characteristic in Fig. 4 has been obtained by averaging the value of the current over one period of the oscillation. As in the experiments, the fine structure of the I-V characteristic appears when additional carriers are introduced by photoexcitation.

The time-resolved current for a fixed voltage of 1.1 is shown in the inset of Fig. 5. The current clearly exhibits periodic oscillations containing higher harmonics. The corresponding frequency spectrum of the oscillating current is also shown in Fig. 5 for a voltage (V=1.1) in the region with negative differential conductivity (NDC). It displays a fundamental frequency of 14 MHz plus higher harmonics with decreasing amplitude, which nicely reproduces the experimental data.

In the absence of photoexcitation, we find undamped current oscillations for appropriate values of the bias only for a doping density ν between 0.04 and 0.15. Below $\nu = 0.04$ the SL evolves from any initial condition to a uniform state with the same constant values of charge and field in each well. Above $\nu = 0.15$ stable electric field domains are formed.[1–3] This limit can also be described by means of a discrete mapping as in Ref. 7. For values in between, we find undamped oscillations in close agreement with the experimental results. The calculated frequency of about 14 MHz does not change much with the applied bias. Within the NDC region, undamped current oscillations are the only stable solution. However, outside this region bistability and hysteresis between the stationary uniform-field solution and the undamped current oscillations are observed. The electric field and charge profiles corresponding to one period of the current oscillation are similar to those found in the undoped case

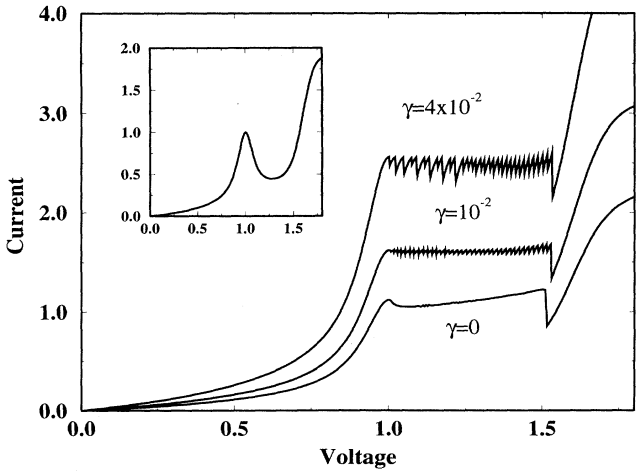

FIG. 4. Calculated I-V characteristic for three different photoexcitation intensities as indicated and $\nu = 0.1$. Inset: Dimensionless $v(E)$ curve used in the simulations. This curve coincides with the I-V characteristic for $\nu < 0.04$.

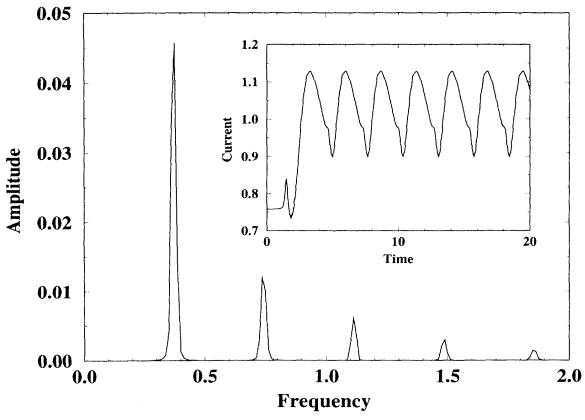

FIG. 5. Current oscillations in real time (inset) and the corresponding Fourier transform for a bias of $V = 1.1$ in the NDC region of the $v(E)$ curve in the inset of Fig. 4, a doping density of $\nu = 0.1$, and photoexcitation density $\gamma = 0$.

(cf. Fig. 9 in Ref. 7). During each period a domain wall (charge monopole) is formed inside the SL. It then moves towards the corresponding contact. Depending on the applied voltage, it may or may not reach the end of the SL before it dissolves and a new monopole is formed starting a new period of the oscillation. Since in a 40-well SL the wall moves only a few wells, it may be hard to distinguish this monopole recycling from a true spatial oscillation of a single monopole. Simulations of longer SL's ($N \geq 100$), however, clearly show monopole recycling with two monopoles coexisting during some part of one current oscillation period. The frequency of the oscillation is mainly determined by the number of wells the monopole moves across and the average drift velocity.[9] In agreement with the experiment the distribution of the amplitudes of the higher harmonics, but not their frequencies, varies strongly with the applied bias.

We have also analyzed the effect of additional photoexcitation on the current oscillations within this model. The amplitude of the oscillations decreases with increasing laser intensity. For large enough intensity, the oscillations disappear as observed in Fig. 3. An important difference between the experimental and calculated result is that in the simulation the oscillation frequency does not depend on the photoexcitation intensity. This discrepancy might be explained by the dependence of the charge accumulation within the first well as a function of the laser power. This has been incorporated into the model by varying the boundary condition δ. The photoexcitation then leads to an increase of the electron density in the SL, thereby diminishing the charge difference between the n^+ region and the SL. As a result the negative charge accumulation in the first well decreases. Taking this effect into account, the calculated oscillation frequency shifts to lower values with increasing laser intensity as observed in the experiments (cf. Fig. 3). The simulated field distributions show that the domain wall is born closer to the first well as δ decreases. Therefore, it has to move over a longer distance during each oscillation period leading to a reduced frequency.

In summary, we have observed and simulated periodic self-oscillations in doped GaAs-AlAs superlattices. These oscillations occur if the number of carriers is large, but not large enough for stable domain formation. The oscillations contain higher harmonics with amplitudes that depend on the applied voltage. The frequency of the oscillations decreases with increasing carrier density until, at very high laser power, the oscillations disappear and the domains become stationary. Using a discrete drift model, it is shown that the oscillations originate from spatial motion of the domain boundary over several periods of the superlattice.

This work was supported in part by the Spanish DGICYT Grant No. PB92-0248 and by the U.S. Army Research Office under Contract No. DAAL-03-92-G-0233. J.G. wishes to acknowledge partial support from MEC-Fulbright and ONR.

[1] L. Esaki and L. L. Chang, Phys. Rev. Lett. **33**, 495 (1974).
[2] K. K. Choi, B. F. Levine, R. Malik, J. Walker, and C. G. Bethea, Phys. Rev. B **35**, 4172 (1987).
[3] H. T. Grahn, R. J. Haug, W. Müller, and K. Ploog, Phys. Rev. Lett. **67**, 1618 (1991).
[4] J. Kastrup, H. T. Grahn, K. Ploog, F. Prengel, A. Wacker, and E. Schöll, Appl. Phys. Lett. **65**, 1808 (1994).
[5] H. T. Grahn, H. Schneider, and K. v. Klitzing, Phys. Rev. B **41**, 2890 (1990).
[6] R. Merlin, S. H. Kwok, T. B. Norris, H. T. Grahn, K. Ploog, L. L. Bonilla, J. Galán, J. A. Cuesta, F. C. Martínez, and J. Molera, in *Proceedings of the 22nd International Conference on the Physics of Semiconductors*, edited by D. J. Lockwood (World Scientific, Singapore, 1995), p. 1039.
[7] L. L. Bonilla, J. Galán, J. A. Cuesta, F. C. Martínez, and J. M. Molera, Phys. Rev. B **50**, 8644 (1994).
[8] H. Le Person, C. Minot, L. Boni, J. F. Palmier, and F. Mollot, Appl. Phys. Lett. **60**, 2397 (1992).
[9] L. L. Bonilla, in *Nonlinear Dynamics and Pattern Formation in Semiconductors and Devices*, edited by F.-J. Niedernostheide (Springer-Verlag, Berlin, 1995), Chap. 5.